doi:10.3772/j.issn.1006-6748.2020.03.008

Research on robust control strategy of single DOF supporting system of MLDSB based on H_∞ mixed-sensitivity Method①

Zhao Jianhua (赵建华)②* ** ***, Chen Tao**, Han Fang**, Gao Dianrong**, Du Guojun*

(* College of Civil Engineering and Mechanics, Yanshan University, Qinhuangdao 066004, P. R. China)

(** Fluid Power Transmission and Control Laboratory, Yanshan University, Qinhuangdao 066004, P. R. China)

(*** Jiangsu Provincial Key Laboratory of Advanced Manufacture and Process for Marine Mechanical Equipment, Zhenjiang 212003, P. R. China)

Abstract

Because of hydraulic-electromagnetic double supporting forms, the supporting capacity and stiffness of magnetic-liquid double suspension bearing (MLDSB) can be improved sharply and then it is more suitable for medium speed, heavy load and frequent-starting occasions. Due to the multiple uncertainty, such as the coupling, the unmodeled dynamics, the parameter perturbation and the external disturbance perturbation, the robust stability and stiffness of control system of MLDSB are hard to meet the design requirements. Firstly, the structural features and the regulation mechanisms of MLDSB are presented and the radial 4-DOF kinetic equations are established. Secondly, the influence factors of the control system's coupling on unbalanced vibration caused by the deviation of the rotor center of mass are revealed, and then the weighting function of suppressing the unbalanced vibration can be obtained. Finally, H_∞ controller of MLDSB is designed with H_∞ mixed-sensitivity method, and the control performances of H_∞ controller is compared with the state feedback controller. The simulation results show that single degree of freedom (DOF) supporting system of MLDSB with H_∞ controller has good robust stability, stiffness and the ability to suppress unbalanced external disturbances. This study can provide the theoretical reference for stabilized suspension and control of MLDSB.

Key words: magnetic-liquid double suspension bearing (MLDSB), single degree of freedom (DOF) supporting system, H_∞ mixed-sensitivity method, state feedback controller, robust stability

0 Introduction

The hydrostatic bearing is introduced into the magnetic levitation to form magnetic-liquid double suspension bearing (MLDSB). And MLDSB is mainly supported by electromagnetic levitation and assisted by hydrostatic, and then its bearing capacity and rigidity can be greatly improved. It's suitable for medium speed, heavy load and the occasions where it is frequently started and the dynamic pressure support is difficult to achieve actual performance [1]. Due to the coupling between electromagnetic system and hydrostatic system and inertia-gyroscopic effect caused by high-speed rotating of the rotor, the model parameter uncertainty and unmodeled dynamic characteristics of MLDSB can be aggravated and the deviations between the real model and the theoretical model are produced, and then the control accuracy and robust control stability can be improved.

Recently, lots of scholars had deeply studied the robust control and suppressing the unbalanced vibration of electromagnetic bearing system and achieved fruitful achievements.

Long et al. [2] established kinetic models of rotor system of 5-freedom electromagnetic bearing and analyzed unbalanced vibration caused by the deviation of the rotor center of mass. The study showed that the robust stability of the rotor system was great and the vibration of rotor could be restrained effectively. Xu et al. [3] established mathematical model of 5-freedom electromagnetic bearing and analyzed the influence of gyroscopic coupling and inertia coupling on the model of the system. Based on sensitivity weighting factor and

① Supported by the National Nature Science Foundation of China (No. 51705445, 52075468), General Project of Natural Science Foundation of Hebei Province (E2020203052), Youth Fund Project of Scientific Research Project of Hebei University (QN202013), Open Project Funding of Jiangsu Provincial Key Laboratory of Advanced Manufacture and Process for Marine Mechanical Equipment and Open Project Funding of Fluid Power Transmission Control Laboratory of Yanshan University.

② To whom correspondence should be addressed. E-mail: zhaojianhua@ysu.edu.cn

Received on Aug. 29, 2019

supplementary sensitivity weighting factor, single degree of freedom (DOF) H_∞ controller and 2-DOF centralized controller with inertial coupling were presented. The results showed that the dynamic and static characteristics of the system were great and the robustness and the ability of restraining disturbance were strong. Gu et al. [4] optimized the design of axial magnetic bearing controller based on mixed sensitivity method H_∞ control. The research shows that single DOF support system of MLDSB with H_∞ controller has a good robust stability, comparatively strong robust and the ability to suppress unbalanced external disturbances compared with traditional PID control. Zhang et al. [5] experimentally researched on the influence of temperature, rotating speed, leakage flux and eddy current on electromagnetic force and solved the contradiction between high rotating speed and high stiffness caused by the complex nonlinearity of the electromagnetic bearing of the electromagnetic bearing grinding machine system. The result showed that high rotating speed and high stiffness can be achieved and the effect of electromagnetic perturbation on the system can be overcome when H_∞ controller is used to control the electromagnetic coil current. Li et al. [6] experimentally studied the electromagnetic bearings-flexible rotor, and the results showed that the rotating speed of the rotor successfully exceeded the second flexible critical speed under robust H_∞ controller, and then the operation accuracy and safety can be improved sharply. Aiming at the interference caused by the mass imbalance of the rotor of electromagnetic bearing, Shang et al. [7] presented a gain-scheduling electromagnetic controller of multi-objective performance requirement. The results showed that electromagnetic bearing system had good robust stability and the ability to restrain unbalanced external disturbance under the action of the controller.

In conclusion, many scholars devoted to unbalanced vibration of flexible rotor and parameter uncertainty of electromagnetic bearing system. However, there are no relevant researches about robust H_∞ control of MLDSB.

When the rotor rotates at high speed, the unbalanced vibration caused by the deviation of mass center can result in the inertia coupling and gyroscopic coupling, and then the robust stability can be reduced sharply. However, robust stability is the basis of the design and operation of MLDSB. Therefore, the dynamic equation of the radial 4-DOF MLDSB system is established, and the uncertainties and its influencing factors caused by the unbalanced vibration are revealed. H_∞ controller is designed with H_∞ hybrid sensitivity method and the control performances of state feedback and H_∞ controller are compared.

1 Mathematical model of MLDSB

1.1 Working principle of bearing system

Eight poles are circumferentially distributed in form of NSSNNSSN in MLDSB. The number of turns of each coil is the same, and 2 adjacent opposite poles are a pair of poles, and the magnetic loop and magnetic force are generated between the magnetic poles and flux sleeve. Inlet hole is processed in each magnetic. As fluid flows through the gaps between the poles and the flux sleeve, large liquid resistance are formed and then the hydrostatic pressure is established on the magnetic pole. After that, static bearing force is generated. Initially, the electromagnetic force and hydrostatic force of each magnetic poles are equal, and two adjacent opposite magnetic pole pairs can be called as supporting unit.

A single DOF supporting system in the vertical direction is taken as an example. Its regulating principle and force diagram are shown as Fig. 1 and Fig. 2. In the initial state, the bias currents of the upper and lower electromagnetic coils are i_0 and the thickness of upper

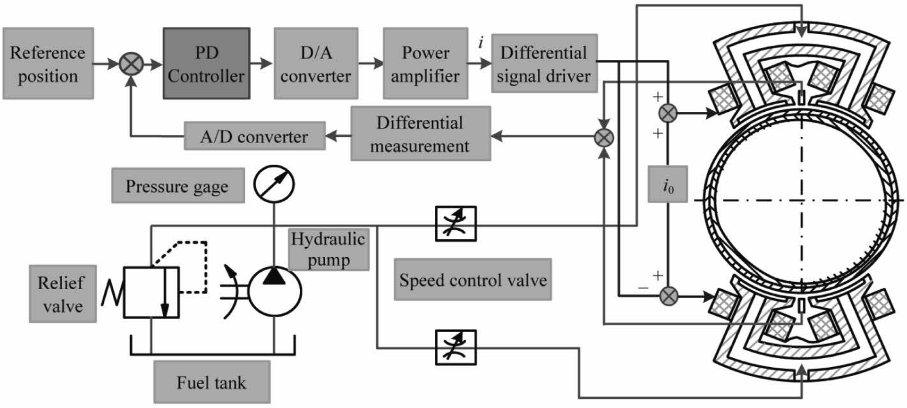

Fig. 1 Single DOF support regulation principle of MLDSB

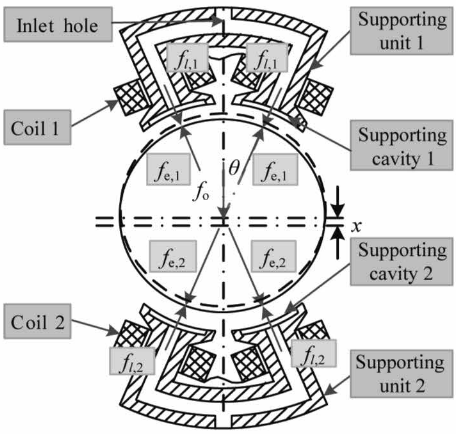

Fig. 2 Force diagram of single DOF MLDSB

and lower oil film are 30 μm. When the external load f acts on the rotor, the displacement of the rotor is x and the thicknesses of the oil films of the upper and lower supporting cavity change, and then the hydrostatic supporting force is generated. The controlling current i_c generated by the electromagnetic system are transferred to the upper and lower coils and then the electromagnetic supporting force is generated. The rotor is adjusted by electromagnetic force and hydrostatic force together so that it can return to the balance position again[8].

1.2 Mathematical model of radial MLDSB

The force diagram of the rotor is shown as Fig. 3, and the meanings of parameters are shown as Table 1.

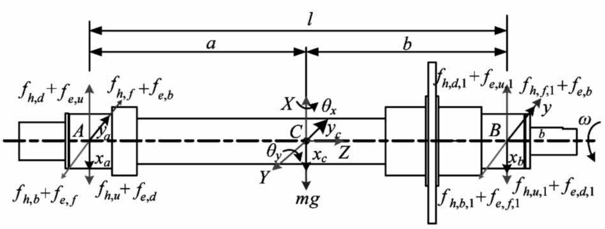

Fig. 3 Rotor of MLDSB

Table 1 Major parameter of MLDSB

Initial bias current i_0	Balance gap of rotor x_0
1.7 A	30 μm

According to Fig. 3, the radial motion equation of the rotor of MLDSB are shown as follows.

$$\begin{cases} m\ddot{x}_c = f_{x1} - f_{x2} + f_{x3} - f_{x4} - f_x \\ m\ddot{y}_c = f_{y1} - f_{y2} + f_{y3} - f_{y4} - f_y \\ M_x = I_r\ddot{\theta}_x + \omega I_a\dot{\theta}_y = (f_{y2} - f_{y1})a + (f_{y3} - f_{y4})b \\ M_y = I_r\ddot{\theta}_y + \omega I_a\dot{\theta}_x = (f_{x2} - f_{x1})a + (f_{x3} - f_{x4})b \end{cases} \tag{1}$$

where, m—— Mass of rotor, kg; $m = 10$;

x_c——X-displacement of mass center, m;
$x_c = (bx_a + ax_b)/l$;
y_c——Y-displacement of mass center, m;
$y_c = (by_a + ay_b)/l$;
x_a——X-displacement of A-end of rotor, m;
y_a——Y-displacement of A-end of rotor, m;
x_b——X-displacement of B-end of rotor, m;
y_b——Y-displacement of B-end of rotor, m;
θ_x——X-angle of rotor, rad; $\theta_x = (y_b - y_a)/l$;
θ_y——Y-angle of rotor, rad; $\theta_y = (x_b - x_a)/l$;
l——Distance between A and B, m; $l = 0.532$ m;
a——Distance between A and mass center, m;
$a = 0.3105$ m;
b——Distance between B and mass center, m;
$b = 0.2215$ m;
ω——Z-rotational speed of rotor, rad/s;
I_r——X-rotational inertia and Y-rotational inertia of rotor, kg·m^2;
$I_r = 0.0225$ kg·m^2;
I_a——Z-rotational inertia of rotor, kg·m^2;
$I_a = 8.85 \times 10^{-4}$ kg·m^2;
M_x——X-torque of rotor, N·m;
M_y——Y-torque of rotor, N·m;
f_x——X-interference, N;
$f_{x1} = f_{h,d} + f_{e,u}$; $f_{x2} = f_{h,u} + f_{e,d}$;
$f_{x3} = f_{e,d,1} + f_{e,u,1}$; $f_{x4} = f_{h,u,1} + f_{e,d,1}$;
f_y——Y-interference, N;
$f_{y1} = f_{h,b} + f_{e,f}$; $f_{y2} = f_{h,f} + f_{e,b}$;
$f_{y3} = f_{e,b,1} + f_{h,f,1}$; $f_{y4} = f_{h,f,1} + f_{e,b,1}$.

The resultant force of magnetic and hydrostatic system can be linearized in the equilibrium position as follows[8].

$$\begin{cases} f_{x1} - f_{x2} = k_r x_a + k_v \dot{x}_a + k_i i_{xa} \\ f_{x3} - f_{x4} = k_r x_b + k_v \dot{x}_b + k_i i_{xb} \\ f_{y1} - f_{y2} = k_r y_a + k_v \dot{y}_a + k_i i_{ya} \\ f_{y3} - f_{y4} = k_r y_b + k_v \dot{y}_b + k_i i_{yb} \end{cases} \tag{2}$$

where, k_r——Displacement stiffness coefficient, N/m;
$k_r = 1.64 \times 10^7$ N/m;
k_v——Velocity stiffness coefficient, N/(m/s);
$k_v = 1.8 \times 10^5$ N/(m/s);
k_i——Current stiffness coefficient, N/A; $k_i = 5100$ N/A;
i_{xa}, i_{xb}——Control current of A-end and B-end along X-axis, A;
i_{ya}, i_{yb}——Control current of A-end and B-end along Y-axis, A;

Take $\boldsymbol{X} = (x_a, x_b, y_a, y_b, \dot{x}_a, \dot{x}_b, \dot{y}_a, \dot{y}_b)^T$ as the state vector, $\boldsymbol{U} = (i_{xa}, i_{xb}, i_{ya}, i_{yb})^T$ as the control vector, and $\boldsymbol{Y} = (x_a, x_b, y_a, y_b)^T$ as the output vector, then the radial state equation of MLDSB system can be obtained as follows.

$$\begin{cases}\dot{\boldsymbol{X}} = \boldsymbol{AX} + \boldsymbol{BU} \\ \boldsymbol{y} = \boldsymbol{CX} + \boldsymbol{DU}\end{cases} \tag{3}$$

where, $\boldsymbol{A}$ is state matrix, $\boldsymbol{B}$ is control matrix, $\boldsymbol{C}$ is output matrix and $\boldsymbol{D}$ is direct transfer matrix.

By substituting Eq. (2) into Eq. (1), the expressions of matrices $\boldsymbol{A}$, $\boldsymbol{B}$, $\boldsymbol{C}$ and $\boldsymbol{D}$ can be obtained as follows.

$$\begin{cases}\boldsymbol{A} = \begin{bmatrix} 0_{4\times4} & I_{4\times4} \\ a_{21} & a_{22}\end{bmatrix} \\ \boldsymbol{B} = \begin{bmatrix} 0_{4\times4} \\ b_{21}\end{bmatrix} \\ \boldsymbol{C} = [I_{4\times4} \quad 0_{4\times4}] \\ \boldsymbol{D} = 0_{4\times4}\end{cases} \tag{4}$$

where, $a_{21} = \begin{bmatrix} a_{11}^{21} & a_{12}^{21} \\ a_{21}^{21} & a_{22}^{21}\end{bmatrix}$; $a_{22} = \begin{bmatrix} a_{11}^{22} & a_{12}^{22} \\ a_{21}^{22} & a_{22}^{22}\end{bmatrix}$;

$$b_{21} = \begin{bmatrix} b_{11}^{21} & b_{12}^{21} \\ b_{21}^{21} & b_{22}^{21}\end{bmatrix};$$

$$a_{11}^{21} = a_{22}^{21} = \begin{bmatrix} \frac{lk_r}{m} + \frac{k_r a^2}{I_r} & \frac{k_r}{m} - \frac{k_r ab}{I_r} \\ \frac{lk_r}{m} - \frac{abk_r}{I_r} & \frac{k_r}{m} + \frac{b^2 k_r}{I_r}\end{bmatrix};$$

$$a_{12}^{21} = a_{21}^{12} = 0_{2\times2};$$

$$a_{11}^{22} = a_{22}^{22} = \begin{bmatrix} \frac{lk_v}{m} + \frac{k_v a^2}{I_r} & \frac{k_v}{m} - \frac{k_v ab}{I_r} \\ \frac{lk_v}{m} - \frac{abk_v}{I_r} & \frac{k_v}{m} + \frac{b^2 k_v}{I_r}\end{bmatrix};$$

$$a_{12}^{22} = a_{21}^{22} = \begin{bmatrix} -\frac{\omega I_a a}{I_r l} & \frac{\omega I_a a}{I_r l} \\ \frac{\omega I_a b}{I_r l} & -\frac{\omega I_a b}{I_r l}\end{bmatrix};$$

$$b_{11}^{21} = b_{22}^{21} = \begin{bmatrix} \frac{lk_i}{m} + \frac{a^2 k_i}{I_r} & \frac{k_i}{m} - \frac{abk_i}{I_r} \\ \frac{lk_i}{m} - \frac{abk_i}{I_r} & \frac{k_i}{m} + \frac{b^2 k_i}{I_r}\end{bmatrix};$$

$$b_{12}^{21} = b_{21}^{21} = 0_{2\times2}.$$

It can be seen from matrix $\boldsymbol{A}$ that the coupling characteristics of MLDSB system are mainly related to the rotational speed and the inertia of the rotor. When the rotational speed is low, the inertial coupling and gyro coupling can be ignored, and then the radial transfer function can be obtained as follows.

$$G(S) = \frac{I(S)}{X(S)} = \frac{k_i}{mS^2 - k_v S - k_r} \tag{5}$$

2 Controller design of MLDSB

2.1 H_∞ mixed sensitivity control

Taking single DOF supporting system as an example, the principle block diagram of the control system is shown as Fig. 4.

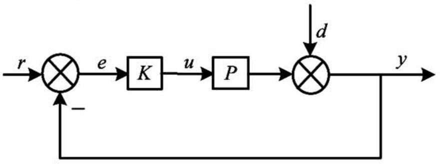

Fig. 4 Principle block diagram of control system

In Fig. 4, r, e, u, d, y, K, P are respectively reference input, tracking error, control quantity, external interference, system output, controller and controlled object. Then the sensitivity function $S(s)$, supplementary sensitivity function $T(s)$ and function $R(s)$ can be obtained respectively as follows.

$$\begin{cases} S(s) = \frac{y}{d} = [I + P(s)K(s)]^{-1} \\ T(s) = \frac{y}{r} = P(s)K(s)[I + P(s)K(s)]^{-1} \\ R(s) = \frac{u}{r} = K(s)[I + P(s)K(s)]^{-1}\end{cases} \tag{6}$$

where, $\| S \|_\infty$ is a measure of the suppression capability to low-frequency interference, $\| T \|_\infty$ is a measure of the suppression capability to high frequency unmodeled dynamic and reappearance capability to reference input, and also the measure of the allowable amplitude Δ of multiplicative perturbation $(I + \Delta)P$. While $\| R \|_\infty$ is the measure of the allowable amplitude ΔG of the additive perturbation $G + \Delta G$ and the suppression capability of the control output[9].

The nominal model $G_0(s)$ is difficult to reflect the actual controlled system. The relationship between actual model and nominal model is $G(s) = G_0(s) + \Delta G(s)$, $\Delta G(s)$ is a bounded perturbation.

According to the robust stability theory, if controller $K(s)$ which can make $G_0(s)$ closed-loop stably exist, for any bounded perturbation $\Delta G(s)$ which can meet $\Delta G(s) \leqslant W_3(s)$, the sufficient condition of the closed-loop stability of the system is shown as follows.

$$| T(s) W_3(s) | \leqslant 1 \tag{7}$$

where, $W_3(s)$ is a supplementary sensitivity weighting function.

For external interference d, $| S(s) W_1(s) | \leqslant 1$ is true by selecting reasonably the sensitivity weight function, and then the closed-loop transfer function can be reshaped in the frequency domain in order to suppress the influence of external interference on system output.

2.2 Controller design and simulation

It can be seen from the state equation of radial MLDSB that the uncertainty includes the parameter uncertainty caused by the linearization of the supporting force and the dynamic uncertainty caused by the inertial coupling and gyroscopic coupling. The uncertainty of parameters is generally caused by the large floating of the rotor, and it includes uncertainty of displacement stiffness coefficient k_x, uncertainty of velocity stiffness coefficient k_v and uncertainty of current stiffness coefficient k_i.

The nonlinear perturbation is the largest when the rotor floats. At this point, $x = 30\ \mu m$, $\dot{x} = 0$, $i = 1.7$ A, and then the multiplicative uncertainty caused by parameter perturbation is $\Delta_1(s)$ as follows.

$$\Delta_1(s) = \frac{s^2 + 127060s - 37320}{10s^2 - 119701s - 2850306} \tag{8}$$

Due to the small pole moment of inertia and rotational speed, the multiplicative uncertainty $\Delta_2(s)$ caused by the inertial coupling can be shown as follows.

$$\Delta_2(s) = \frac{1.2s^2 + 130102s - 38012}{9.8s^2 - 120110s - 2798403} \tag{9}$$

The expression of same frequency centrifugal interference caused by the eccentricity of the rotor is $F_d = m\varepsilon\omega^2\cos\omega t$, eccentric distance is $\varepsilon = 5\ \mu m$ [10]. So displacement amplitude of the rotor caused by disturbance can be obtained as follows.

$$|d| = \left|\frac{F_d}{(m(j\omega)^2 - k_x)}\right| \tag{10}$$

Due to the highest rotational speed (6 000 r/min) of MLDSB, the corresponding interference amplitude can be obtained as follows.

$$|d| = 9.4 \times 10^{-6}\cos(618t) \tag{11}$$

In order to ensure that the radial amplitude x_m of the rotor does not exceed one tenth of the radial gap of the bearing (30 μm), so the maximum amplitude of expected sensitivity function $S(s)$ can be obtained when $\omega_1 = 618$ rad/s as follows.

$$|S(j\omega)| = 20\lg\left|\frac{x_m}{|d|_{\max}}\right| \tag{12}$$

So radial transfer function of MLDSB can be obtained as follows.

$$P_0(s) = \frac{5100}{10s^2 - 1.8 \times 10^5 s - 1.64 \times 10^7} \tag{13}$$

It can be seen from Eq. (13) that $P_0(s)$ contains an unstable pole. In order to suppress the low frequency noise, the inverse of the sensitivity weighting function $W_1(s)$ should be greater than $S(j\omega_1)$ near ω_1 position, So $W_1(s)$ can be expressed as follows.

$$W_1(s) = \frac{1000}{s + 10} \tag{14}$$

To eliminate greater saturation in order to prevent damaging the equipment and increasing the order of the controller, $W_2(s)$ is usually assumed as a scalar quantity.

$$W_2(s) = 0.0002 \tag{15}$$

Since the supplementary sensitivity weighting function W_3 is related to the bandwidth of the system, the dominant pole of MLDSB is 90.65/s and the bandwidth can be identified as 80 rad/s, and then W_3 and its singular value can be shown as follows.

$$W_3(s) = \frac{5000(s + 20)(s + 15)}{(s + 1500)(s + 2500)} \tag{16}$$

It can be seen from Fig. 5 that the singular value W_3 is above $\Delta_1(s)$ and $\Delta_2(s)$, so the overflow phenomenon of the controller can be avoided to obtain good control effect.

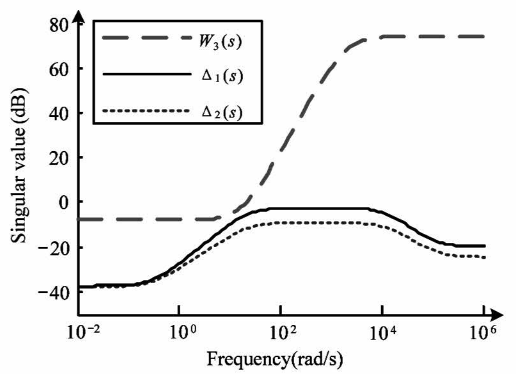

Fig. 5 Curves between W_3 and singular value

By using Matlab software, transfer function $K(s)$ of H_∞ controller can be obtained as follows.

$$K(s) = \frac{T_4 s^4 + T_3 s^3 + T_2 s^2 + T_1 s + T_0}{s^4 + \Gamma_3 s^3 + \Gamma_2 s^2 + \Gamma_1 s + \Gamma_0} \tag{17}$$

where, $T_4 = 60.6$, $T_3 = 5.472 \times 10^5$, $T_2 = 4.813 \times 10^8$, $T_1 = 9.612 \times 10^{10}$, $T_0 = 2.751 \times 10^{12}$, $\Gamma_3 = 3.831 \times 10^4$, $\Gamma_2 = 2.681 \times 10^7$, $\Gamma_1 = -3.911 \times 10^9$, $\Gamma_0 = 1.479 \times 10^{10}$.

The singular value characteristics of the weighting function of complementary sensitivity function $T(s)$, sensitivity function $S(s)$ are shown as Fig. 6 and Fig. 7.

It can be seen from Fig. 6 and Fig. 7 that reciprocal of supplementary sensitivity weighting function $1/W_3(s)$, reciprocal of sensitivity weighting function $1/W_1(s)$ are respectively above complementary sensitivity function $T(s)$ and sensitivity function $S(s)$. Meanwhile, $W_1(s)$ has low connectivity and its cut-off frequency is less than that of $W_3(s)$, so $W_1(s)$ can satisfy the requirement of weighting function[11,12].

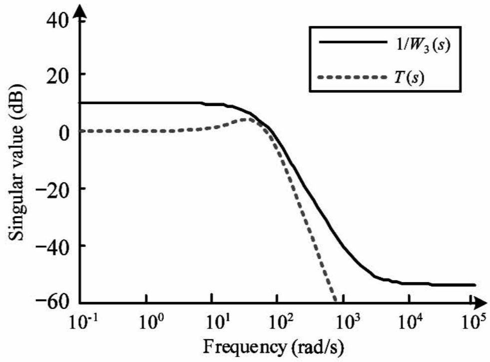

Fig. 6 Complementary sensitivity function and singular value characteristics of its weighting function

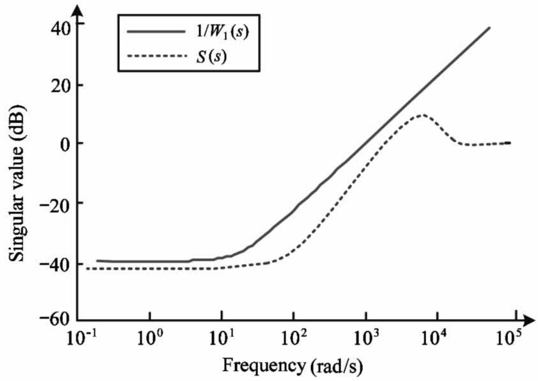

Fig. 7 Sensitivity function and singular value characteristics of its weighting function

By using Matlab\Simulink simulation tool, the floating characteristic curve (step signal, amplitude is 1 μm) of single DOF support system can be presented as Fig. 8.

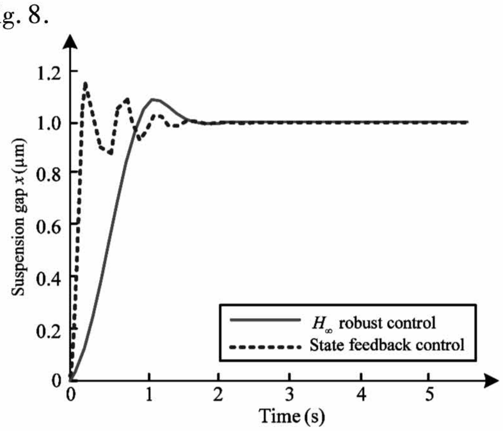

Fig. 8 Floating characteristic curve of suspension clearance

It can be seen from Fig. 8 that adjustment time and overshoot of single DOF supporting system with H_∞ mixed sensitivity controller are both smaller than that with the state feedback controller[12,13].

When the rotor is supported stably at the rotating center, its floating characteristic curve under the situation that 500 N pulse interference is suddenly added at $t = 3$ s can be shown as Fig. 9.

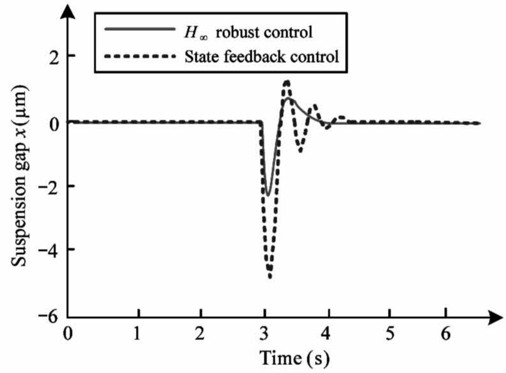

Fig. 9 Floating characteristic curve of pulse external excitation interference suspension clearance

It can be seen from Fig. 9 that the offset distances under H_∞ mixed sensitivity control[14,15] and under the state feedback control are 2 μm and 5 μm respectively.

The floating characteristic curve of suspension clearance is shown as Fig. 10 when amplitude is 500 N and frequency is 100 Hz.

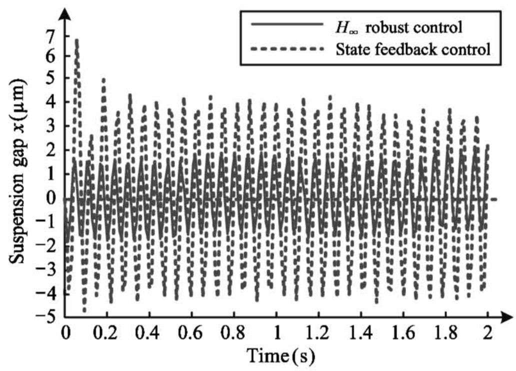

Fig. 10 Floating characteristic curve of sine external interference suspension clearance

It can be seen from Fig. 10 that the amplitude of the rotor under H_∞ hybrid sensitivity control is 1.5 μm (a tenth of the radial gap length) while 7 μm under state feedback control. To sum up, single DOF support system of MLDSB with H_∞ controller has good dynamic[16], robust stability and the ability to suppress unbalanced external disturbances.

3 Conclusion

The mathematical model of radial MLDSB system is established, the uncertainty of controlled object is evaluated based on H_∞ hybrid sensitivity optimal control theory, and the weighted function is obtained.

MLDSB with H_∞ hybrid sensitivity control has good dynamic characteristics, stiffness, robust stability and vibration suppression ability.

References

[1] Zhao J H, Wang Q, Zhang B, et al. Influence of liquid film thickness on static property of magnetic-liquid double suspension bearing[C]// International Conference on Intelligent and Interactive Systems and Applications, Beijing, China, 2017: 809-816

[2] Long Y W, Wei Z J, et al. Research on H_∞ robust control for strategy magnetic bearing [J]. *Vibration and Shock*, 2013, 32(23): 9-14

[3] Xu L X, Zhang J M, Yu T Z. Research on the application of H_∞ control theory in magnetic levitation bearing system[J]. *China Mechanical Engineering*, 2006, 17 (10): 1060-1064 (In Chinese)

[4] Gu G X, Lu Y J, Deng Z Q. An axial magnetic bearing controller based on H_∞ control theory[J]. *Power Automation Equipment*, 2002, 22(12): 51-54

[5] Zhang Q C, Xing T, Li G D. Research on the controller of motorized spindle in electromagnetic bearing grinder system[J]. *Journal of Mechanical Engineering*, 2006, 42(11): 168-172

[6] Li H W, Xu Y, Gu H D. The maneuver balancing method on electromagnetic bearings in the flexible rotor system [J]. *China Mechanical Engineering*, 2008, 19 (12): 1419-1422 (In Chinese)

[7] Shang A L, Ma W M, Liu D Z. Multi-objective controller design for electromagnetic bearing gain scheduling[J]. *Control and Decision*, 2009, 24(3): 403-407

[8] Zhao J H, Chen T, Wang Q, et al. Stability analysis of single DOF supporting system of magnetic-liquid double suspension bearing[J]. *Hydromechatronics Engineering*, 2019, 47(6): 1-7

[9] Qiu X, Xu J X, Xu Y, et al. A new differential evolution algorithm for minimax optimization in robust design[J]. *IEEE Transactions on Cybernetics*, 2017, (14): 1-14

[10] Gao H, Xu L X. Analysis on beat vibration in active magnetic levitation bearing system[J]. *Journal of Mechanical Engineering*, 2011, 47(13): 104-112

[11] Wu X D, Xie X S. Weighted array selection in H_∞ robust control[J]. *Journal of Tsinghua University*, 1997 (1): 27-30

[12] Lu S G, Jiang S Y. μ robust control of electromagnetic bearing[J]. *Journal of Mechanical Engineering*, 2007, (1): 137-142

[13] Xing T, Zhang Q C, Liang Y C. H_∞ robust fuzzy controller design of electromagnetic bearing[J]. *Journal of Harbin University of Technology*, 2006, 38(1): 11-14

[14] Liu F C, Gao J F, Li Q. Adaptive robust control of flexible-joint space manipulators under different gravity environments[J]. *High Technology Letters*, 2015, 25(1): 21-24 (In Chinese)

[15] Tang Z H, Wu M, Gui W H. Decentralized robust control of robot systems based on LMI approach[J]. *High Technology Letters*, 2000,10(8): 76-79 (In Chinese)

[16] Yang G J, Geng W J, Li H W, et al. Study on the relationship about magnetic bearings rotor structure and natural frequency for 10MW high temperature gas-cooled reactor[J]. *High Technology Letters*, 2003, 13(4): 72-76 (In Chinese)

Zhao Jianhua, born in 1983. He is currently an associate professor at School of Mechanical Engineering, Yanshan University, China. He received his B. S. degree in 2006, M. S. degree in 2010, Ph. D degree in 2013 from Yanshan University, China. His research interests include simulation and analysis of hydrostatic bearing, magnetic-liquid double suspension bearing system.